M.Sc Project Report on

Synthesis and characterization of YBCO Thick Films

Submitted by
Ankita Paul
(411PH2110)

Under the guidance of

Prof. D.Behera

Department of Physics
National Institute of Technology
Rourkela - 769008

NATIONAL INSTITUTE OF TECHNOLOGY ROURKELA

DEPARTMENT OF PHYSICS

CERTIFICATE

This is to certify that the project report entitled "**Synthesis and Characterization of YBCO Thick Films**" is submitted by **Miss Ankita Paul** in partial fulfillment of the requirement towards the award of Master of Science degree in Physics at **NIT, Rourkela**. This is an authentic work carried out by her under my supervision and guidance in low temperature laboratory of the Department of Physics.

To the best of my knowledge, the matter embodied in the thesis has not been submitted to any other University/Institution.

Prof. D. Behera
Department of Physics
NIT Rourkela

ACKNOWLEDGEMENT

On the submission of my thesis report titled as "**Synthesis and characterization of YBCO thick films**", I would like to thank our guide Prof **D. Behera** for his patience and his helpful discussion with me during the course of my work for the l year. I would like to thank **Miss Arpna Kujur**, for sharing ideas with me and helping in my project work.

I give sincere gratitude to Department of Metallurgical and Material Science for extending all facilities to carry out the **XRD** and **SEM**.

I express heartiest thanks to all the faculty members of Department of Physics, NIT Rourkela who have made contributions towards the completion of this project.

It gives me an immense pleasure to thank all our friends and all the research scholars of the Dept. of Physics, NIT Rourkela for their constant inspiration.

Thank you

Ankita Paul

(411ph2110)

ABSTRACT

Thick films of (1-x) YBCO + x Y_2O_3 (x= 0, 5, 10, 15, 20 wt. %) composites are prepared using diffusion reaction. Microstructural analysis is performed using SEM, and phase conformation of YBCO composite is done by X-ray diffraction method. Data collected are computer controlled through automated programs. XRD of pristine YBCO has orthorhombic phase at room temperature with space group Pmmm, but with the increase in the concentration of Y_2O_3, impurity peaks were observed. The resistivity vs. temperature was done by four probe method. It is found that by increasing the wt. % of Y_2O_3 in YBCO matrix, transition temperature (T_c) gradually decreases, and for very high concentration, a semiconducting trend was observed with a drop in resistivity.

List of Contents

Introduction

1.1 General remarks:

The electrical resistivity of many metals and alloys drops suddenly to zero when the specimen is cooled to sufficiently low temperature, often a temperature in the liquid helium range this phenomena is called superconductivity, was observed first by kammerlingh ones in 1911 in Leiden.

Superconductors:

Superconductor is a material that loses all resistance to the flow of electric current when it is cooled below a certain temperature, called the *critical temperature* or *transition temperature*. Above this temperature there is usually little or no indication that the material might be a superconductor. Below the critical temperature, not only does the superconductor suddenly achieve zero resistance, it gains other unusual magnetic and electrical properties. Two fundamentally important and intuitively startling properties are associated with superconductivity are as follows:

- Superconductors above T_c has a finite resistance, below T_c their resistivity becomes zero that is conductivity becomes infinity.
- The magnetic susceptibility of superconductors changes from small positive paramagnetic value to X= -1, that is below T_c they become perfectly diamagnetic.

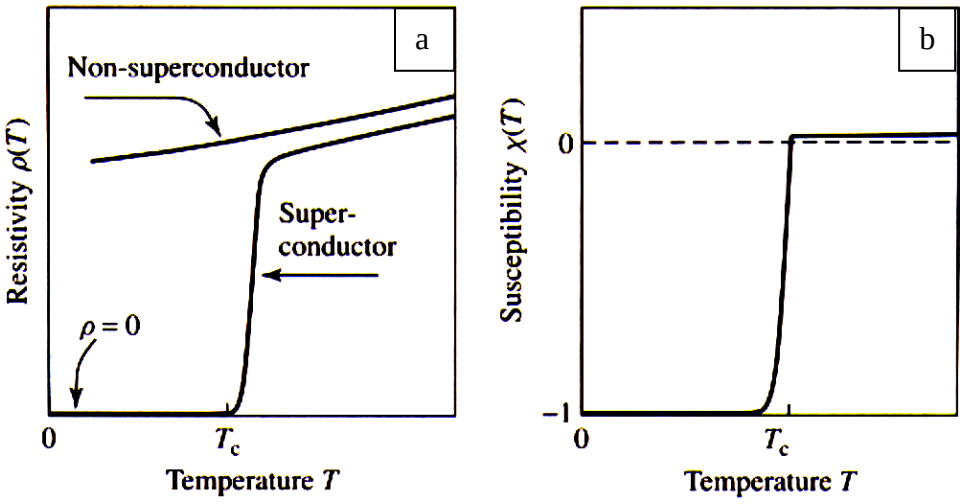

Figure1. (a) We see that the superconducting sample in its transition temperature has zero resistivity $\rho = 0$ as compared to non superconducting sample. (b) Shows the behavior of susceptibility which drops to minus one below Tc. The onset of the diamagnetic response corresponds quite closely to the point where $\rho \rightarrow 0$ on the temperature axis. The figure also indicates that χ is positive but quite small above Tc.

1.2 Types of superconductors

Depending upon their behavior in an external magnetic field, superconductors are divided into two types:

(**1) Type I superconductors**:

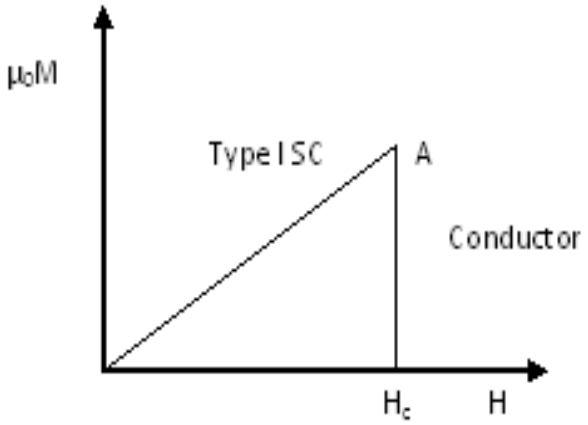

Figure 1: M-H diagram of Type I superconductor.

a). Type I superconductors are those superconductors which lose their superconductivity very easily or abruptly when placed in the external magnetic field. As you can see from the graph of intensity of magnetization (M) versus applied magnetic field (H), when the Type I superconductor is placed in the magnetic field, it suddenly or easily loses its superconductivity at critical magnetic field (H_c) (point A).After H_c, the Type I superconductor will become conductor.

b). Type I superconductors are also known as **soft superconductors** because of this reason that is they lose their superconductivity easily.

c) Type I superconductors perfectly obey Meissner effect.

d) Example of Type I superconductors: Aluminum (Hc = 0.0105 Tesla), Zinc (H_c = 0.0054)

(2) **Type II superconductors**:

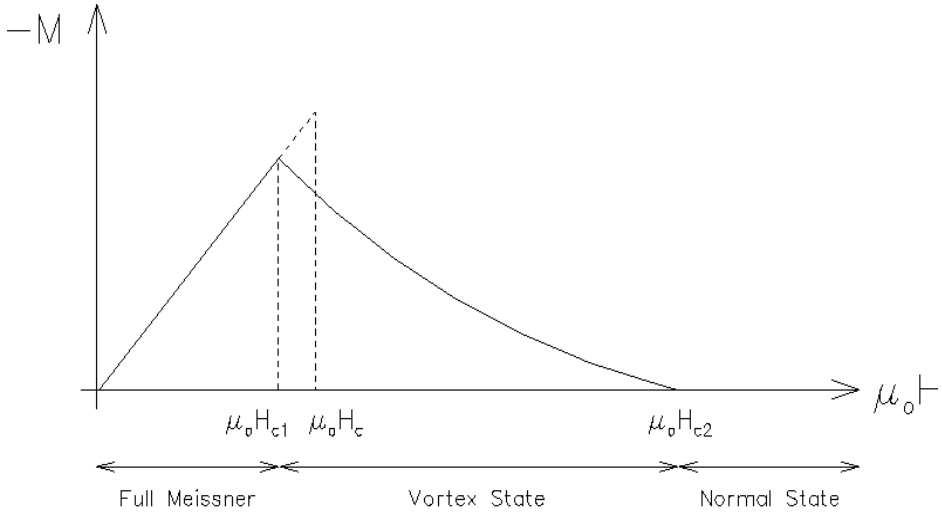

Figure 3: M-H diagram of Type II superconductor.

a). Type II superconductors are those superconductors which lose their superconductivity gradually but not easily or abruptly when placed in the external magnetic field. As you can see from the graph of the intensity of magnetization (M) versus applied magnetic field (H), when the Type II superconductor is placed in the magnetic field, it gradually loses its superconductivity. Type II superconductors start to lose their superconductivity at lower critical magnetic field (Hc1) and completely lose their superconductivity at upper critical magnetic field (Hc2).

b) The state between the lower critical magnetic field (Hc1) and upper critical magnetic field (Hc2) is known as vortex state or intermediate state. After Hc2, the Type II superconductor will become a conductor.

c) Type II superconductors are also known as **hard superconductors** because of this reason that is they lose their superconductivity gradually but not easily.

d) Type II superconductors obey Meissner effect but not completely.

e) Type II superconductors are used for strong field superconducting magnets.

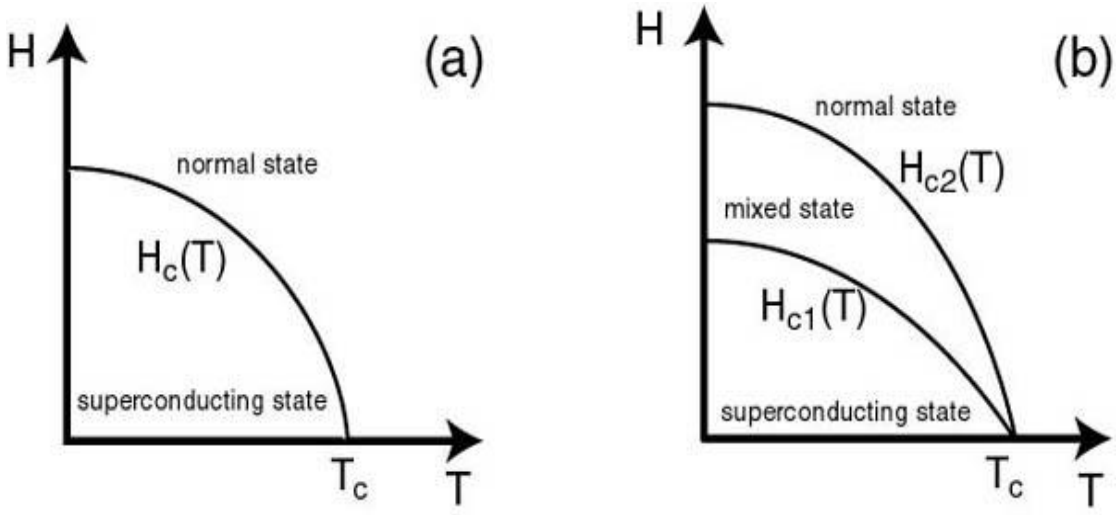

Figure 4: Critical magnetic field at (a) normal and (b) superconducting states.

1.3 Properties of superconductors

- **MEISSNER EFFECT**

In 1933 meissner and ochsenfeld measured the flux distribution outside tin and lead specimens which had been cooled below their transition temperatures while in a magnetic field. They found that at their transition temperatures the specimens spontaneously become perfectly diamagnetic, cancelling all flux inside even though they have been cooled in a magnetic field. When a superconductor is cooled in a weak magnetic field, at their transition temperature persistent current arise on the surface and circulate so as to cancel the flux density inside, in just the way as the magnetic field is applied when the metal has been cooled. This effect, where by superconductor never has a flux density even when in a applied magnetic field is called meissner effect. This property has implications for making high speed, magnetically-levitated trains, for making powerful, small, superconducting magnets for magnetic resonance imaging, etc.

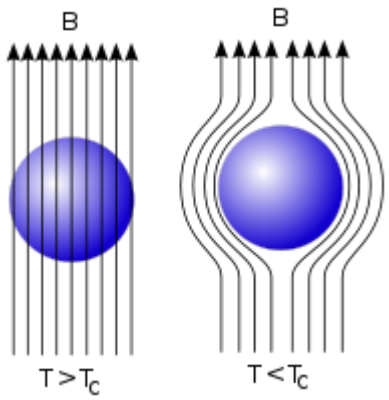

Figure 5: Diagram of Meissner Effect. Magnetic field lines represented as arrows excluded from a superconductor when it is below its critical temperature.

- **JOSEPHSON EFFECT**

When two superconductors are separated by a very thin insulating layer, quite unexpectedly, a continuous electric current appears, the value of which is linked to the characteristics of the superconductors. This effect was predicted in 1962 by Brian Josephson. Since then, this superconductor-insulator-superconductor sandwich has been called a “Josephson

junction". This effect has implications for superfast electrical switches that can be used to make small, high-speed computers.

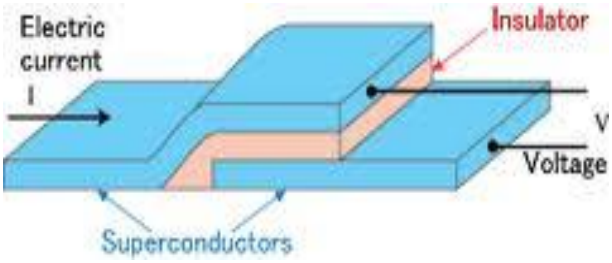

Figure 6: Josephson's Effect in a superconductor –insulator- superconducting junction

- **SPECIFIC HEAT**

The specific heat of the normal metal is seen to be of the form,

$C_n(T) = \alpha T + \beta T^3$

The first term in the above equation is the specific heat of electrons in the metal and the second term is the contribution of the lattice vibration at low temperatures. The specific heat of superconductors shows a jump at T_c since superconductivity affects electrons mainly so lattice vibration part remains unaffected and we find that the electronic specific heat is nonlinear with temperature.

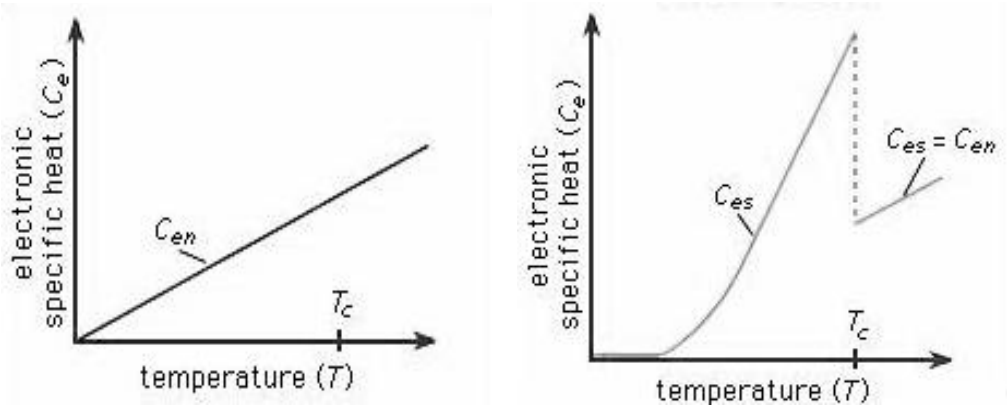

Figure 7: Temperature dependence of the electronic specific heat in the normal and superconducting states.

- **SUPERFLUIDITY**

This phenomenon is closely related to Bose Einstein condensation. Super fluidity was first observed in liquid helium. Helium at these low temperatures was seen to flow quite freely, without any friction, through any gaps and even through very thin capillary tubes. When helium is cooled to a critical temperature (called its lambda point), a remarkable discontinuity in heat capacity occurs, the liquid density drops, and a fraction of the liquid becomes a zero viscosity "superfluid". Superfluidity, the frictionless flow and other exotic behavior observed in liquid helium at temperatures near absolute zero (−273.15 °C, or −459.67 °F), and (less widely used) similar frictionless behavior of electrons in a superconducting solid.

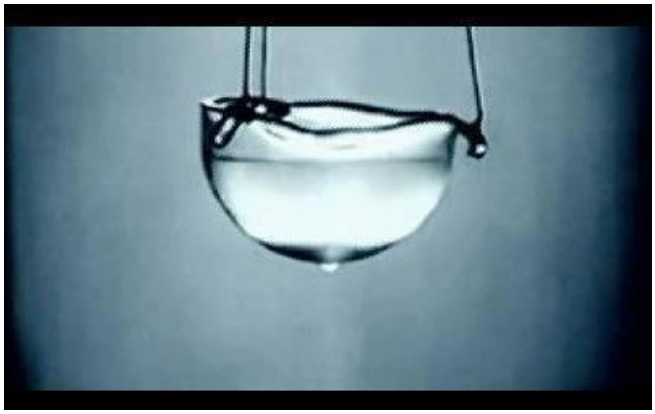

Figure 8: Liquid helium in the superfluid phase.

- **CRITICAL FIELD**

In superconductors, their normal resistance may be restored if a magnetic field greater than the critical value H_c is applied to the specimen. Hc depends both on the material and on the temperature (T). It tends to H_0 as T tends to 0 K. In general for higher values of H_c the Tc value is lower and vice versa.

- **CRITIICAL CURRENT DENSITY**

An electric current is always associated with a magnetic field. Hence if a superconductor carries a current such that the field which it produces is equal to Hc, then the resistance of the

sample will be restored. The current density at which it occurs is called the critical current density.

BCS THEORY:

The microscopic theory put forward by Bardeen, Cooper and Schrieffer (BCS), in 1957 provides the better quantum explanation of superconductivity and accounts very well for all the properties exhibited by the superconductors. This theory involves the electron interaction through phonons as mediators. The fundamental idea underlying BCS theory is that electrons pair up with one another due to a special type of attraction (interaction). These pairs of electrons are called copper pairs. Normally two electrons repel each other. However, the electrons could attract each other via distortion of the lattice. The idea is if we consider an electron passing close to an ion, there will be a momentary attraction between them which might slightly modify the vibrations of the ion. This in turn could interact with a second electron nearby which will also be attracted to the ion. But net effect of these two interactions is that there is an apparent attractive force between the two electrons and this would not have arisen if the ion had not been present. The BCS theory is able to explain all the properties shown by the superconductor.

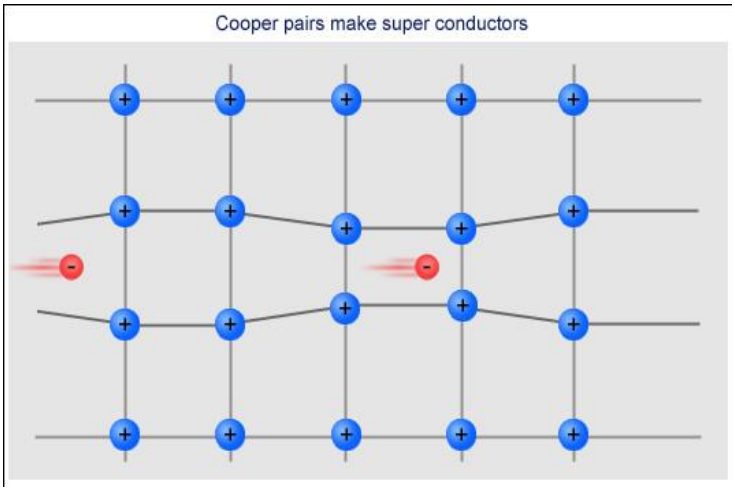

Figure 9: Flow of Cooper pair through the lattice.

1.4 YBCO Superconductors

Superconductivity has wide applications in many fields including energy storage, electrical power transmission, high speed trains, large physics machines, optoelectronics magnetic levitation, magnetic shielding etc. so, there is always a demand for materials having superconducting properties, which also should be less expensive and better then the former one. Synthesizing a superconducting material having transition temperature close to room temperature is a major challenge for the scientists. Heading towards this path the current Focus of much of the research, development and commercialization of superconductors is on YBCO.

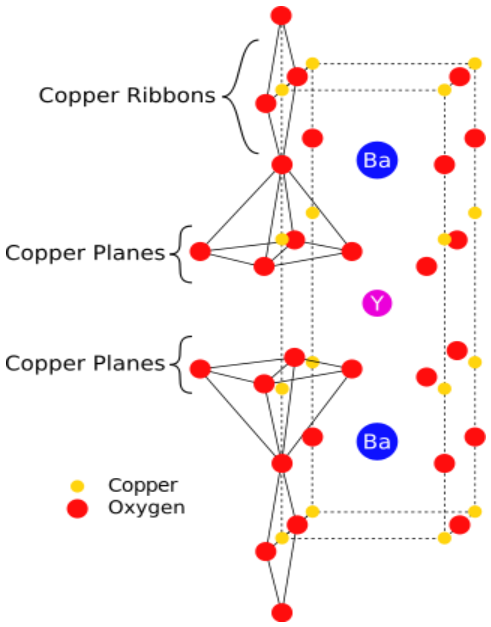

Figure 10: Structure of YBCO.

The discovery of a YBCO superconducting material in 1987 brought about a great excitement within the scientific community. The idea that a material can conduct electricity free of resistance, at temperatures above 77 K, the temperature at which nitrogen liquefies, opened up the possibility for numerous advancements in electronics and wire technologies. The development of such devices, however, turned out to be a very difficult task. Among the major barriers are the inherent brittleness of YBCO and the high processing temperature required to produce the superconducting phase. It has a Penetration depth of 120 nm in the ab plane, 800 nm along the c axis and Coherence length of 2 nm in the ab plane, 0.4 nm along the c axis. YBCO has a defective perovskite structure with layers. The boundary of each layer

is defined by planes of square planar CuO_4 units sharing 4 vertices. The planes can sometimes be slightly puckered. Perpendicular to these CuO_2 planes is CuO_4 ribbons sharing 2 vertices. The yttrium atoms are found between the CuO_2 planes, while the barium atoms are found between the CuO_4 ribbons and the CuO_2 planes. This structural feature is illustrated in the figure to the right. Another important aspect of YBa2Cu3O7-δ material is that, like the other cuprates has an isotropic behavior, as a consequence of its crystalline structure that is reflected in the directional dependence of λ, ξ & Hc2.The anisotropy of these parameters is remarkable between the c-direction & the a or b direction, while the anisotropy between the a & b direction is small & can be neglected in most cases. The anisotropy of HTS materials can be described using Ginzburg- Landau theory that introduces a different effective mass of the hole carriers in different directions.

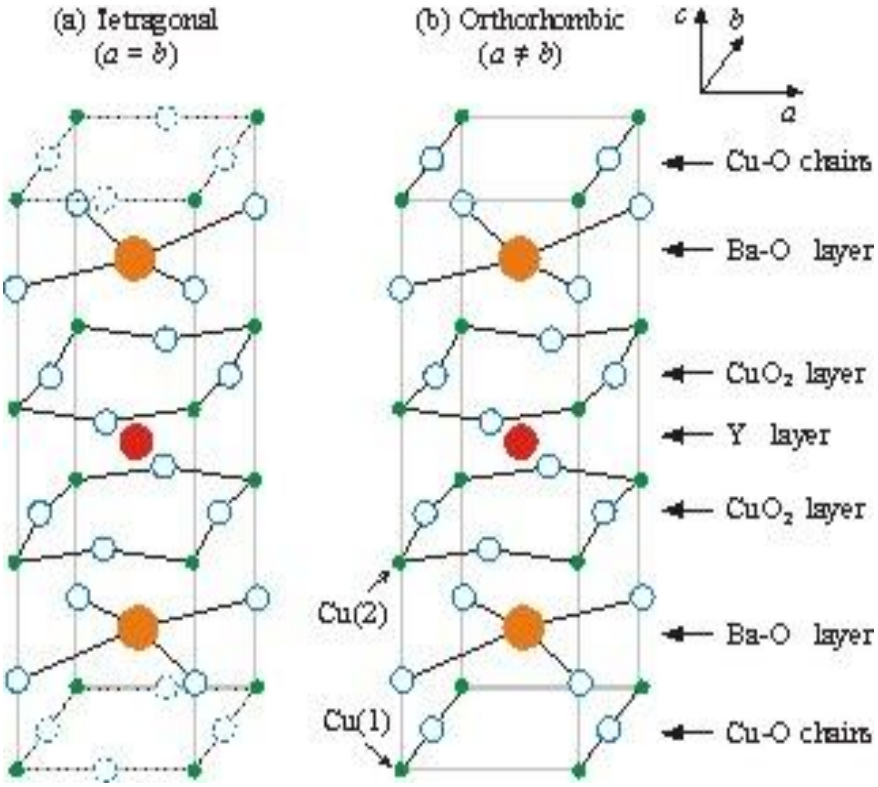

Figure 11: Tetragonal and Orthorhombic Structure of YBCO.

1.5 Motivation of using Y_2O_3

The motivation of choosing Y_2O_3 to make composite with YBCO is because of its promising flux pinning property. Flux Pinning is a phenomena to enhance the critical current density in High Temperature Superconductors by somehow arresting the movement of fluxons. The low critical current density is largely a consequence of an undesired phenomenon called Flux Creep, the ease with which magnetic vortices can move. The motion of these fluxons creates a pseudo-resistance which depresses both critical current density and critical field, thereby limiting the technological applications of High Temperature Superconductors. Moreover Y_2O_3 is chemically non reactive with YBCO and has a close lattice mismatch of 0.6%. The small lattice mismatch allows epitaxial growth of Y_2O_3 nanoparticles in YBCO matrix, which in turn, yields a composite thin film with very low intrinsic strain.

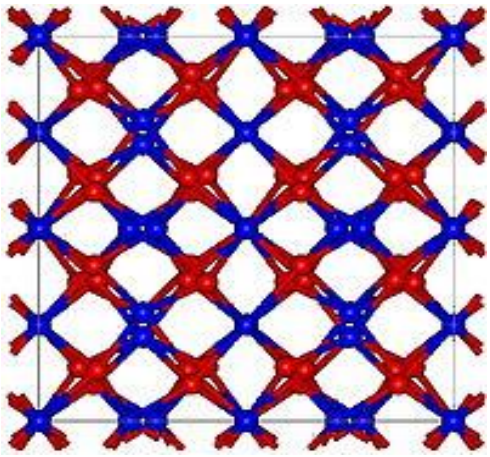

Figure 12: Structure of Y_2O_3.

2. Sample preparation

YBCO superconducting thick films were prepared on Y211 substrate using the diffusion reaction of the coating layer of $Ba_3Cu_5O_8$ on the surface of the substrate. The different steps involved in the film preparation are as follows:

1. Preparation of the substrate
2. Preparation of the paste for coating the substrate.
3. Deposition of the paste on the substrate
4. Optimizing of the sintering schedule for the formation of the superconducting film.

Y211 substrate was prepared by solid state reaction route involving the chemical equation.

$$Y_2O_3 + BaCO_3 + CuO \longrightarrow Y_2BaCuO_5 + CO_2$$

The precursor powders were mixed thoroughly in an agate mortar and pestle, and calcined at 850^0C for 30 hours with 4 intermediate grindings. Then the calcined powders were reground for 1 hour. After grinding final pellets were made by applying pressure and were sintered at 920^0C for 24 hours.

The powders of $BaCO_3$ and CuO were mixed in the stoichiometric ratio of 3:5 to form $Ba_3Cu_5O_8$ for the preparation of the paste for coating the substrates**.**

$$3BaCO_3 + 5CuO \longrightarrow Ba_3Cu_5O_8 + 3CO_2$$

The homogeneously mixed powders were sintered at 850^0 C for 48 hours with three intermediate grindings. $Ba_3Cu_5O_8$ powder thus obtained were finely ground in a mortar and pestle and mixed with an organic solvent polyethylene glycol to make a thick paste for deposition on the substrate. $Ba_3Cu_5O_8$ would diffuse through a few layers of Y_2BaCuO_5 substrate to form $YBa_2Cu_3O_7$ (~ thickness12 μm) superconducting film as:

$$Y_2BaCuO_5 + Ba_3Cu_5O_8 + 1/2O_2 \longrightarrow 2YBa_2Cu_3O_7$$

After confirmation of phase of YBCO thick film, we proceeded for composite preparation. $Ba_3Cu_5O_8$ powder was mixed with different weight percentage of Y_2O_3 (5, 10, 15, 20 wt %) and were finely ground in agate mortar for 2 hours. The ground powder was well mixed with polyethylene glycol to prepare a paste. Care has been taken to maintain the viscous flow of the paste. Using a glass slide the paste is dragged over the Y211 substrate such that a uniform coating of black paste covers the substrate. The substrates with the over layer of varying concentration of Y_2O_3 (5, 10, 15, 20 wt %) is placed inside a furnace at 200^0 C for drying followed by sintering at 920^0 C for 12 hr such the final stage of diffusion occurs. The sample

is annealed at 500 C for 12 hours in oxygen supply such that the samples do not have oxygen deficiency.

Heating profile:

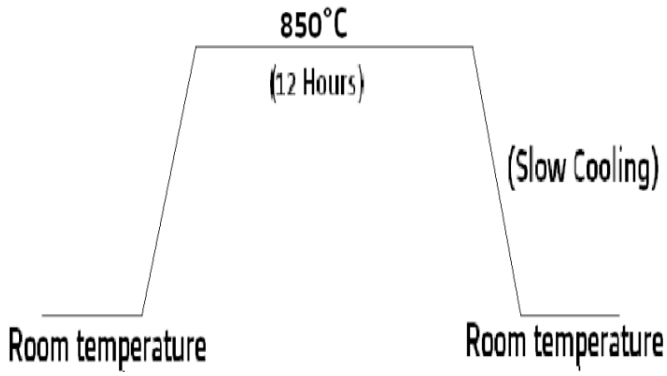

Figure 13: Heating profile for calcination.

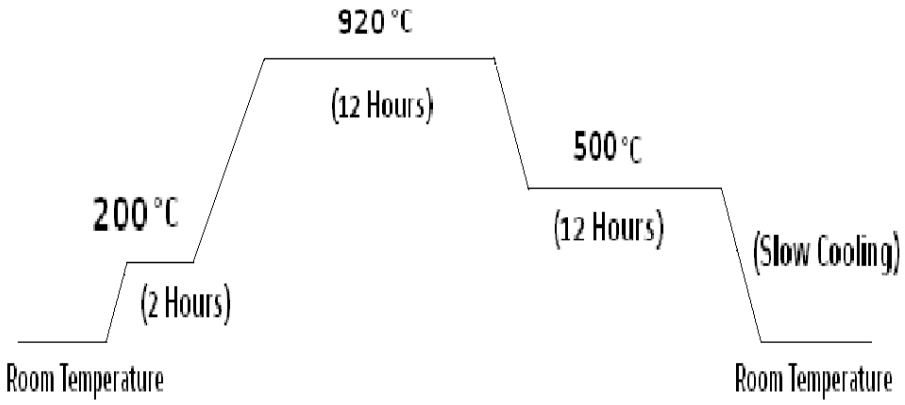

Figure 14: Heating profile for sintering.

Preparation Flowchart:

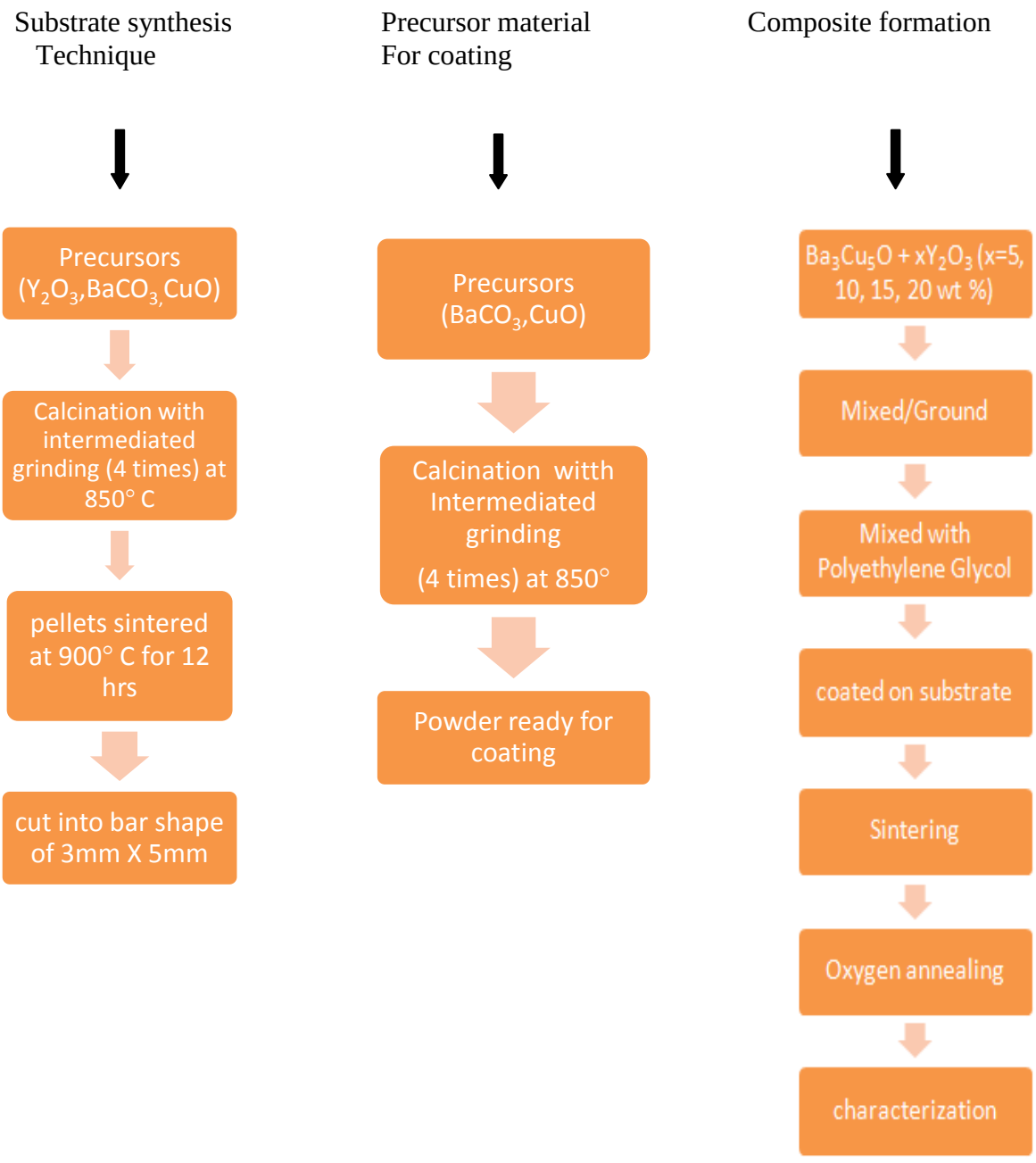

3. Characterization tools:

2.1 LOW TEMPERATURE R-T MEASURMENT BY FOUR PROBE METHOD:

The Four Probe Method is one of the standard and most widely used methods for the measurement of resistivity of semiconductors. In its useful form, the four probes are collinear. The error due to contact resistance, which is especially serious in the electrical measurement on semiconductors, is avoided by the use of two extra contacts (probes) between the current contacts. In this arrangement the contact resistance may be high compare to the sample resistance, but as long as the resistance of the sample and contact resistances are small compared with the effective resistance of the voltage measuring device (potentiometer, electrometer or electronic voltmeter), the measured value will remain unaffected. The setup uses a four probe configuration. The most accurate lead wire configuration is the 4-wire configuration. In a true 4- wire configuration, the resistance of the lead wires does not contribute to the resistance of the sensor.

The true 4-wire measurement uses the current-potential method. A current of known value (I+) passes through the sensor along the "current" lead wires. The voltage generated across the sensor is measured using the "potential" lead wires and the sensor's resistance is calculated by dividing the measured voltage by the Known current. The resistance of the lead wires is not a factor because the value of the current is equal at any point in the circuit. It is independent of the resistance of the lead wire and the input impedance of the voltage measurement circuitry is high enough to prevent any significant current flow in the voltage leads. Since no current is flowing, the voltage along the potential leads does not change along their length.

The voltage drop is measured between the two probes by means of a Keithley 2182A Nano voltmeter and current was measured by Keithley 6221 AC and DC Current Source. The Lake Shore Model 332 Temperature Controller creates was used for temperature measurement. The Model 332 offers high resolution with negative temperature coefficient (NTC) resistance temperature detectors (RTDs) to temperatures as low as 1 K.

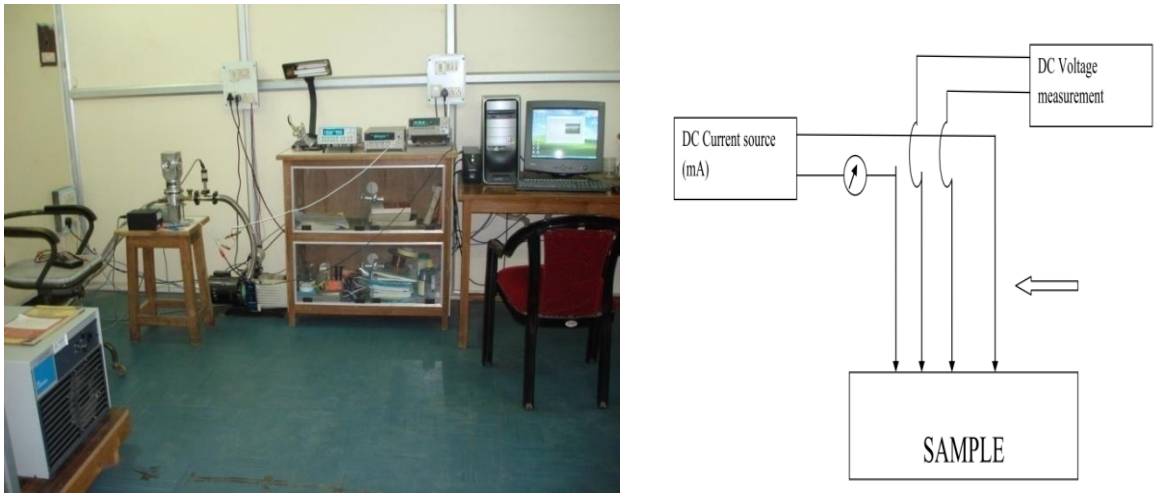

Figure 15: Four probe set up for resistance measurement.

2.2 X-RAY DIFFRACTION:

X-ray diffraction (XRD) is one of the methods we can use to identify the structures of crystalline solids. The XRD patterns are somewhat like fingerprints in that they are unique to each material. The information in an XRD pattern is a direct result of two things; the size and shape of the unit cells, which determine the relative positions of the diffraction peaks. Atomic positions within the unit cell, which determine the relative intensities of the diffraction peaks. This technique is based on the basic principle that a parallel monochromatic X-ray beam of wavelength 'λ' incident at an angle of θ is diffracted by a set of parallel planes of a crystal (Fig.), which is governed by Bragg's law:

$$2d \sin \theta = n\lambda$$

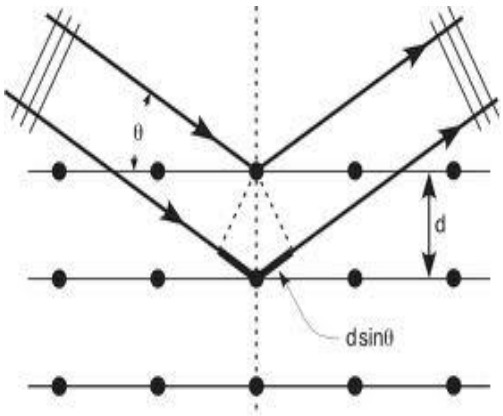

Figure 16: Bragg's Diffraction

X-ray diffractometers consist of three basic elements: an X-ray tube, a sample holder, and an X-ray detector. X-rays are generated in a cathode ray tube by heating a filament to produce electrons, accelerating the electrons toward a target by applying a voltage (36kV), and bombarding the target material with electrons. When electrons have sufficient energy to dislodge inner shell electrons of the target material, characteristic X-ray spectra are produced. X-ray diffraction constitutes current of 20mA. As the sample and the detector are rotated, the intensity of the reflected X-rays is recorded. When the geometry of the incident X-rays impinging the sample satisfies the Bragg Equation, constructive interference occurs and a peak in intensity occurs. A detector records and processes this X-ray signal and converts the signal to a count rate which is projected on the computer screen.

2.3 SCANNING ELECTRON MICROSCOPE (SEM):

The scanning electron microscope (SEM) is a type of electron microscope that takes images of the surface of samples by focusing a high energy beam (~15kV) of electrons onto the sample. The electrons interact with the atoms that make up the sample producing signals that give information about the sample. Electronic devices are used to capture or detect these signals and either allow them to expose film or, most common today, create an image on a computer screen. The type of signals made by an SEM can include secondary electrons, characteristic x-rays, and back scattered electrons. In an SEM, these signals come from the beam of electrons striking the surface of the specimen and interacting with the sample at or near its surface. SEM has allowed researchers to examine a much bigger variety of specimens. The scanning electron microscope has many advantages over traditional microscopes. The SEM has a large depth of field, which allows more of a specimen to be in focus at one time. The SEM also has much higher resolution (4500), so closely spaced specimens can be magnified at much higher levels. Because the SEM uses electromagnets rather than lenses, the researcher has much more control in the degree of magnification. All of these advantages, as well as the actual strikingly clear images, make the scanning electron microscope one of the most useful instruments in research today. SEM micrographs have a very large depth of focus yielding a characteristic three-dimensional appearance useful for understanding the surface structure of a sample. Characteristic x-rays are the second most common imaging mode for an SEM. These characteristic x-rays are used to tell the chemical

composition of the sample. Back-scattered electrons (BSE) that come from the sample may also be used to form an image.

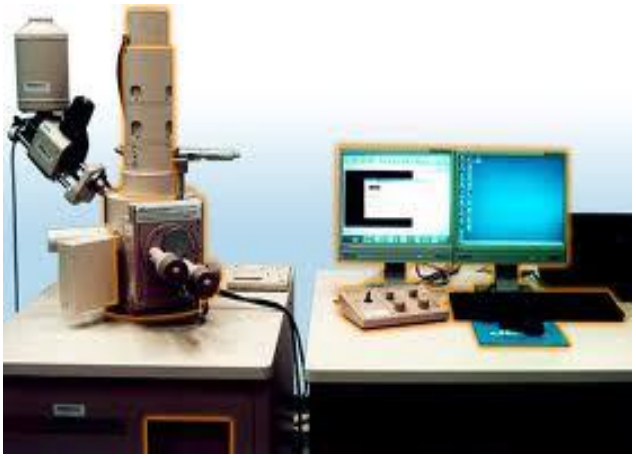

Figure 17: SEM Setup

4. Results and Discussion:

1. Structure analysis by XRD

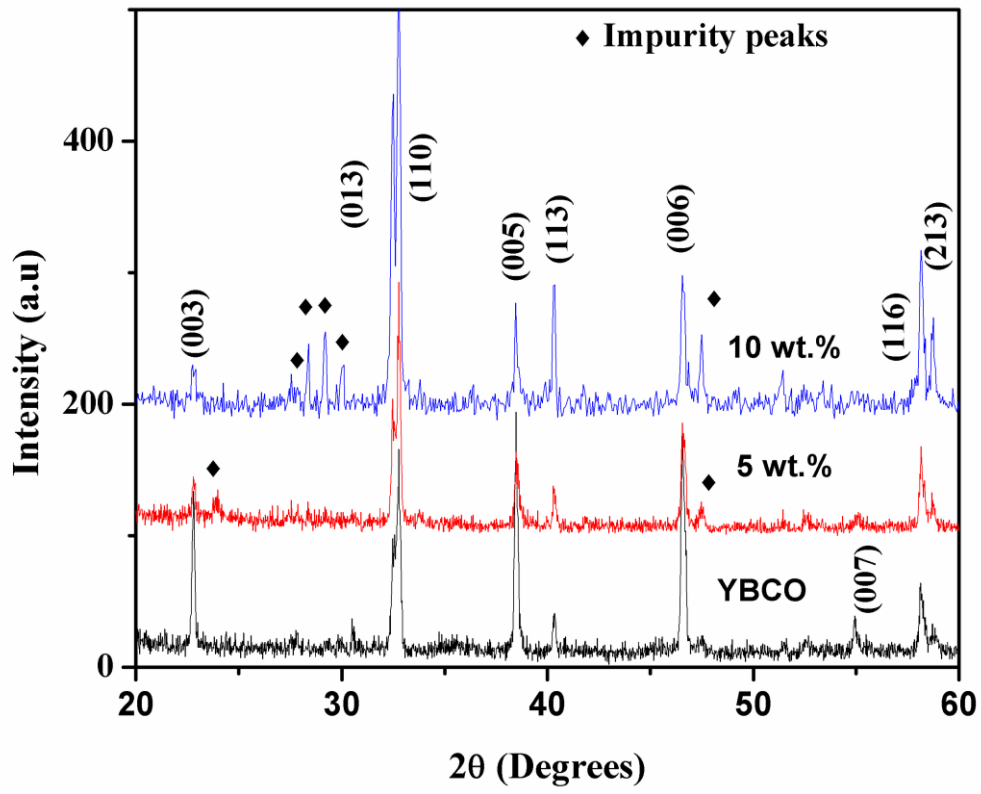

Figure 18: XRD graph of YBCO+ xY_2O_3 (x= 0, 5, 10 wt. %) composites.

Figure 16 shows diffraction pattern of samples. Well defined peaks are noted. The patterns are indexed with Chekcell software and the phases were confirmed to be orthorhombic at room temperature with a space group P*mmm*. Appearance of peaks (003), (005), (006) and (007) in the XRD pattern reveals (00*l*)-orientation of YBCO. Non (00*l*) peaks are seen in the figure. We observe a net decrease in intensity but no shift in 2θ values. However increase in full width half maxima is also revealed in the peak indexed with (013) and (110). As the wt % of Y_2O_3 is increased, impurity peaks were observed so XRD of further high wt % composites was not taken.

4.2 Morphological Analysis by SEM:

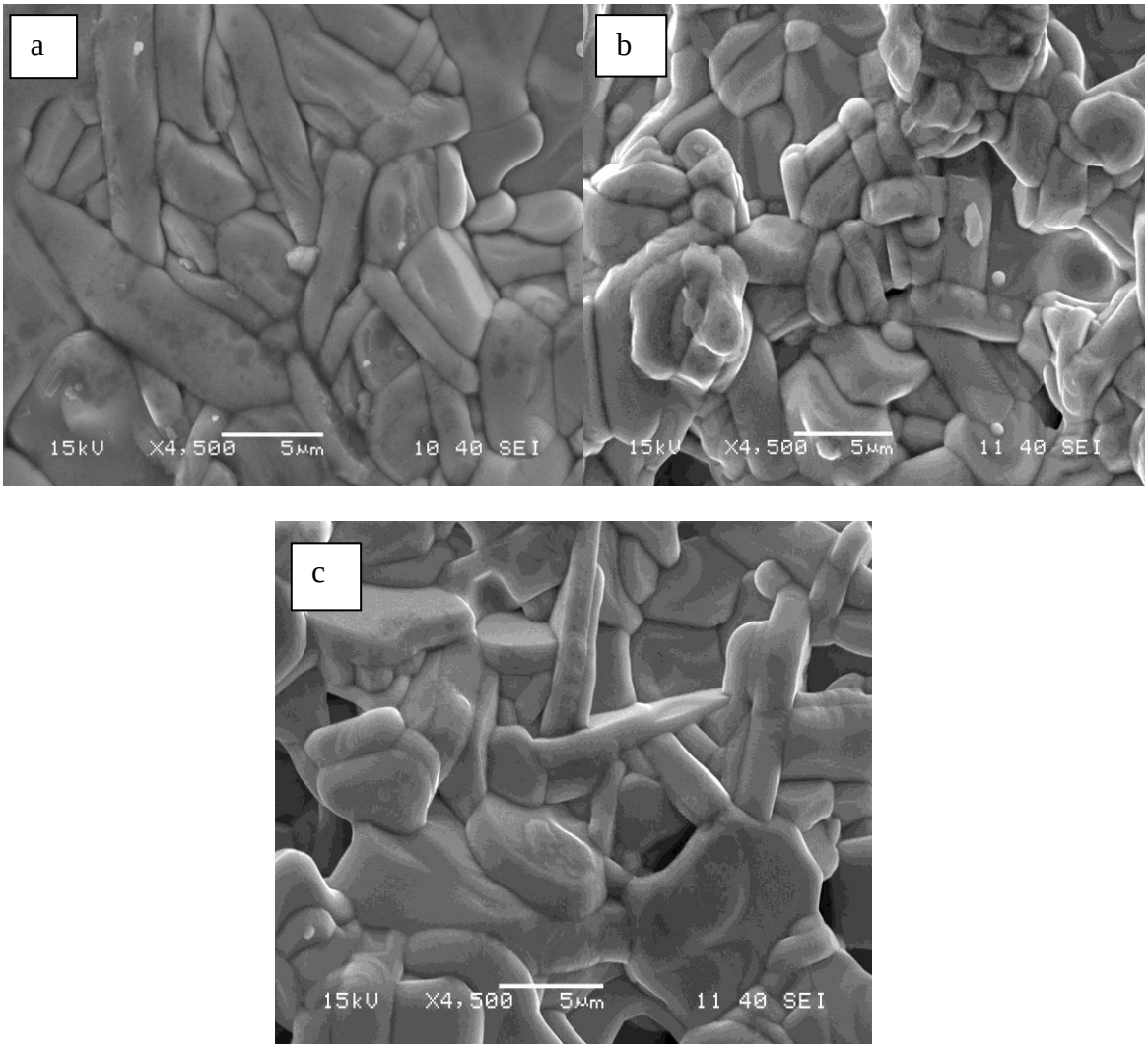

Figure 19: Scanning Electron Microscope of (a) YBCO, (b) YBCO+5 wt. % Y_2O_3, (c) YBCO+10 wt. % Y_2O_3.

The microstructure characterization, i.e. grain-size distribution in the superconductor composites is linked to transport properties. It shows that the pristine YBCO sample exhibits large tube like grains with size varying from 1 to 5 µm in length. With Y_2O_3 addition of 5 wt% of Y_2O_3, grain size reduced and become disoriented which is evident in the figure.

4.3 DC electrical resistivity by four probe technique:

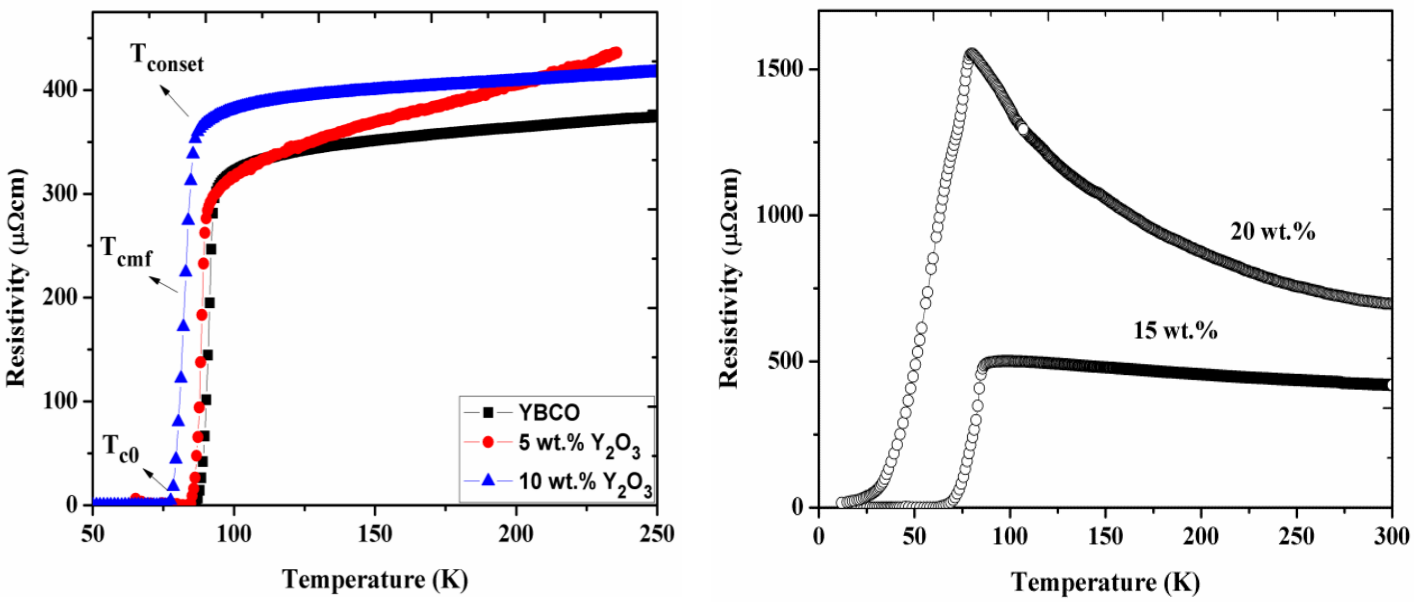

Figure 20: Temperature dependence resistivity plot.

The figure 18 Shows the temperature dependent resistivity for composite sample (1-x) YBCO+ xY_2O_3, where x (5, 10, 15, 20 wt. %.). The graph exhibit two regions- One being linear at temperature above 2Tc and the region characterized by non linearity. The linearity regime represents metallic character and the devation in linearity marks the presence of two kinds of charge carriers i.e. superconducting electrons and the normal charge carriers. Sizeable information drawn from the the plot are (i) the room temperature resistivity increases with Y_2O_3 addition for all concentration. (ii) With the addition of 15 and 20 of Y_2O_3 inclusions to YBCO matrix a semiconducting trend can be clearly seen followed by a drop. (iii) However, 20 wt. % of non superconducting 3D artificial pinning agent does not destroy the flow of supercurrent but the intergranular modifications add to broadening of transition width. (iv) 5 wt. % of Y_2O_3 when added to YBCO causes appreciable decrease in resistivity as to comparatively pristine and higher concentrated Y_2O_3 added samples. Further we have fitted the normal state resistivity with the relation $\rho_n (T) = \rho_0 + \alpha T$. ρ_0 represents residual resistivity obtained from extrapolation of linear fitting of resistivity to 0 K. ρ_0 show a regular increasing trend as function Y_2O_3 addition but 5 wt. % Y_2O_3 composite records lower value than pristine. This may be due to enhancement of weak link interconnectivity and addition of charge carriers to charge conduction layer.

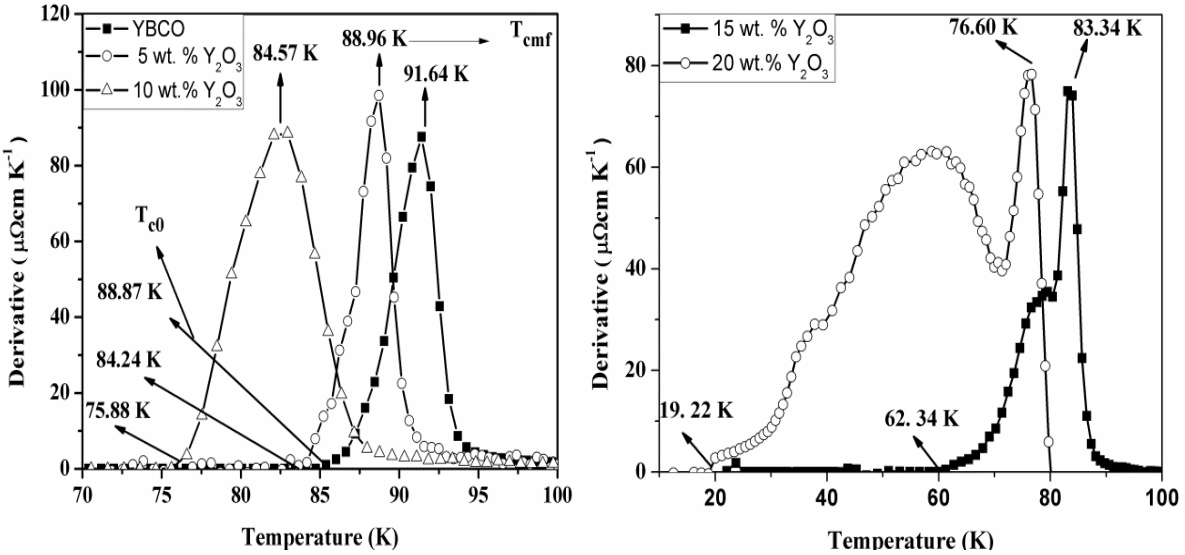

Figure 21: Temperature derivative of resistance plot.

Temperature derivative plot of resistivity portrays additional information to superconducting parameters. Temperature derivative shows a sharp peak or marks a sharp change resistivity called as mean field transition temperature (Tcmf). Our pristine YBCO sample records Tcmf ~ 91.64 K. The concentration of Y_2O_3 plays a crucial role in varying the different superconducting parameters T_{cmf}, T_{onset} and the zero global resistivity (T_{c0}). An increment in the transition width is noted for mixing of Y_2O_3 to YBCO. A remarkable feature of peak bifurcation is shown for higher conc of Y_2O_3 (15 and 20 wt. %). Figure (19) shows a sharp peak followed by shoulder or bump with broader transition width. A second peak appearance is a clear indication of secondary phase present in the YBCO matrix. T_{c0} analysis shows a drastic decrease in achievement of zero resistivity state. T_{c0} is highly intergranular linked parameter affected by defects, vacancy, intersistial and addition of chemical pressure etc.

Table 1: The various parameters associated with transition T_{c0}, T_{cmf}, T_{conset} and ρ_0 (Residual resistivity)

Conc. Of Y_2O_3	T_{c0} (K)	T_{cmf} (K)	T_{conset} (K)	Slope	ρ_0 (μΩcm)
0	88.87	91.64	94.52	0.219	319.89
5	84.24	88.96	90.61	0.77	251.20
10	75.88	84.57	87.87	0.17	374.12
15	62.54	83.34	86.55	-	-
20	19.89	76.60	80.04	-	-

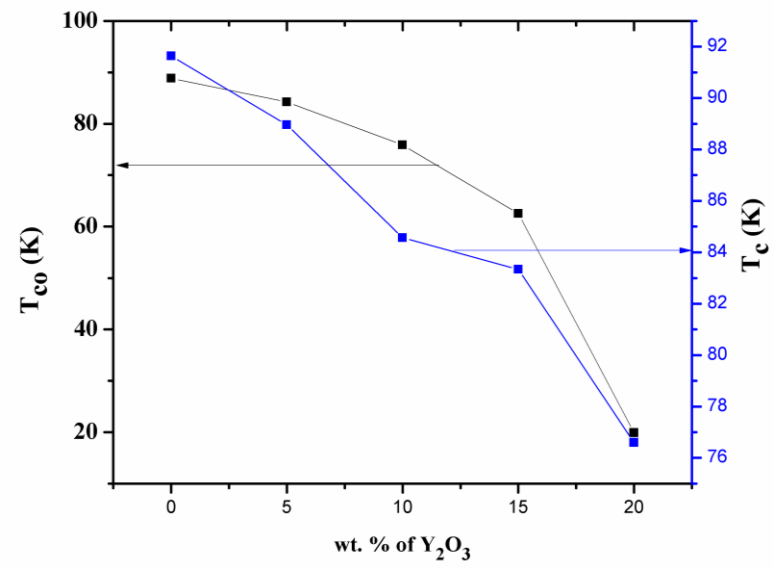

Figure 22: T_{c0} and T_c v/s wt. % Y_2O_3.

Superconductivity which begins within the grains (intragranular regions) is relatively unaffected byY_2O_3 but the progressive coupling of intergrain boundaries via weak link produces intergranular disturbances and electronic modification responsible for reduction of T_{c0}. The various parameters are evaluated and compiled in table 1. Figure (20) shows a plot of T_{c0} and T_c with different concentration of Y_2O_3. It depicts the clear decreasing trend of T_{c0} and T_c with increasing weight. % Y_2O_3.

5. Conclusion

The role of well known Y_2O_3 non superconducting inclusion in YBCO matrix is studied. Y_2O_3 having a close lattice mismatch with YBCO shows up as an impurity peak at 5 wt. % in the XRD pattern on additional to YBCO. Undoubtedly with higher concentrations, the impurity also increases as shown by 10 wt. % XRD pattern. Well oriented grains with a grain size lower than 5 μm is confirmed from morphology. The inference from DC electrical resistivity reveals the following characteristics: The room temperature resistivity increases with Y_2O_3 wt. % addition with a signature of decrease in transition temperature and onset global resistivity. The sharp change in the trend of resistivity for 15 and 20 wt. % of Y_2O_3 are noted to be semiconducting followed with a fall in resistivity as the temperature is further lowered. The main findings of this work give an outlook of 'what amount of Y_2O_3 wt. % can be used for artificial pinning centers'. We conclude from our analysis that Y_2O_3 can be varied from 5 wt. % to 10 wt. % to be added as artificial pinning centers to YBCO for enhancement of critical current density as 15 and 20 wt. % of Y_2O_3 records semiconducting rise in resistivity.

References

[1] Knizhnik, A (2003). "Interrelation of preparation conditions, morphology, chemical reactivity and homogeneity of ceramic YBCO". Physica C: Superconductivity

[2] M. K. Wu, J. R. Ashburn, C. J. Torng, P. H. Hor, R. L. Meng, L. Gao, Z. J. Huang, Y. Q. Wang, and C. W. Chu (1987). "Superconductivity at 93 K in a New Mixed-Phase Y-Ba-Cu-O Compound System at Ambient Pressure". Physical Review Letters

[3] F. Xu*et al.* (1998). "Surface Coordination Chemistry of $YBa_2Cu_3O_7$-δ". *Langmuir*

[4] Li-Chun Liáng. YBCO Superconductor Research Progress

[5] Stephen J. Blundell. Superconductivity: A Very Short Introduction

[6] Charles P. Poole, Jr., Horacio A. Farach, Richard J. Creswick. Superconductivity

[7] J Bardeen, LN Cooper, JR Schrieffer (1957). "Theory of Superconductivity" Physical Review– APS

[8] P Gennes (1989). Superconductivity of metals and alloys

[9] A A Gapud, D Kumar, S KViswanathan, C Canton , MVarela, J Abiade, S J Pennycook and D K Christen. "Enhancement of flux pinning inYBa2Cu3O7−δ thin films embedded with epitaxially grown Y2O3 nanostructures using a multi-layering process".
Institute of physics publishing, Superconductor science and technology.

[10] S.K. Viswanathan , A.A. Gapud , M. Varela , J.T. Abiade , D.K. Christen S.J. Pennycook , D. Kumar. "Enhancement of critical current density of YBa2Cu3O7 − δ thin films by self-assembly of Y2O3 nanoparticulates". Elsevier

[11] Fumitake Kametani, Zhijun Chen, Alex Gurevich and David Larbalestier
Applied Superconductivity Center, National High Magnetic Field Laboratory, Florida State University, Tallahassee, FL32301. "Microstructural Study of Strong Vortex Pinning in a Coated Conductor for Use in Specific Fields and Temperatures".

[12] M. Tinkham, Phys. Rev. Lett. 61 (1988) 1658.

[13] N. Pompeo, V. Galluzzi, A. Augieri, F. Fabbri, G. lentano, T. Petrisor, R. Rogai, E. Silva, IEEE/CSC & ESAS European Superconductivity News Forum. 3 (2008).

[14] H. Padma Kumar, C. Vijay Kumar, J. Alloys Compd. 458 (2008) 528.